Proceedings of the 2003 IEEE International Frequency Control Symposium and PDA Exhibition
Jointly with the 17th European Frequency and Time Forum

THE PIEZOELECTRIC SEMICONDUCTOR AND ACOUSTOELECTRONIC DEVICE DEVELOPMENT IN THE SIXTIES

Fred S. Hickernell
Motorola Inc. (ret.) and The University of Central Florida
Phoenix, Arizona and Orlando, Florida

Abstract - In the 1960's the properties of piezoelectric semiconductors, group III-V zinc-blende and group II-VI wurtzite structure, were explored for the development of acoustoelectronic, (AE), devices. Bulk acoustic wave, (BAW), delay lines, traveling wave amplifiers, and oscillators were developed. Although these elegant functional devices never made it into the realm of full-scale production and application, the piezoelectric semiconductor developments of the 1960's provided an exciting time for theoretical explanations and creative experimentation to explore device capabilities for electronic systems applications. Delay lines were formed from rectangular parallelepiped blocks of piezoelectric semiconductors with integral input and output transducers depleted of carriers at each end of the block. The ultrasonic traveling wave amplifier was based on the interaction of electrons under a bias field moving with a velocity faster than the piezoelectric field accompanying the acoustic traveling wave. The gain factor in a piezoelectric semiconductor under direct current bias was used to develop oscillators. This historical presentation will be illustrated by experimental work done at Motorola in the period from 1962 to 1969 to introduce piezoelectric semiconductor components and devices into electronic systems.
Keywords – piezoelectric semiconductors, delay lines, amplifiers, oscillators, CdS, CdSe, GaAs, ZnO.

I. Introduction

The 1960's could be characterized by the competing technologies of the so-called functional analog device developments and the continuing advances being made in integrated digital circuits. Many believed the basic solution to achieving the required electronic functions was not by building structures composed of classical circuit elements, but by utilizing physical interactions in matter to accomplish the function as directly as possible. J. A. Morton of Bell Telephone Laboratories wrote, " *The aim of electronics is not simply to reproduce physically the elegance of circuit mathematics – rather, it is to perform desired electronic system functions as directly and as simply as possible from the basic structure of matter*." The electronic functions that could be accomplished by utilizing the properties of piezoelectric semiconductors were such an approach. It was prompted by the basic theoretical and experimental work at Bell Telephone Laboratories starting in the early 1960s. The story represents an example of the growth of a technology from certain basic scientific discoveries to their application as solid-state electronic components in advanced prototype electronic systems under development during the sixties. The sixties were a time when acoustic wave devices received greater attention because of the properties of piezoelectric semiconductors.

The general outline of this paper will be the following. First, the properties of four of the most common piezoelectric semiconductors used in the development of acoustoelectronic (AE) devices, CdS, CdSe, GaAs, and ZnO, will be described. Next the development of diffusion layer transducers in a piezo-semiconductor, which allowed the generation and detection of high frequency acoustic waves in a block of crystal, is illustrated. The basic equations regarding the attenuation and velocity dispersion of acoustic waves in piezoelectric semiconductors are then considered. In the presence of a biasing dc electric field the electrons traveling in a piezo-semiconductor will interact with the electric field accompanying the propagating acoustic wave causing it to attenuate or to grow depending upon the strength of the dc field. This gave rise to a second important device, the ultrasonic traveling wave amplifier. The third device was the piezo-oscillator with current oscillations from moving acoustic domains under the action of a dc field, whose period was determined by crystal length. Thus three device classes, unique to piezoelectric semiconductors, were under development in industry and government laboratories during the sixties. The paper is concluded and acknowledgments and references given. The references allow tracing of the historical developments.

II. The Properties of Piezoelectric Semiconductors

The piezoelectric semiconductor occupies a rather unique position among materials used in solid-state electronic devices. As a piezoelectric it can be used to generate and detect acoustic waves. As a semiconductor it can be used as a junction device for performing diode and transistor type functions. As a piezoelectric semiconductor it embodies traveling wave electron-phonon interactions, which permit the development of active acoustoelectronic devices such as amplifiers and oscillators.

Table 1 lists approximate representative values of the piezoelectrically-active device-related acoustic and semiconductor properties of the four crystals that were commonly investigated. The acoustic velocities, phonon attenuation, electromechanical coupling factor, resistivity

range, and mobility are shown. The first three crystals, zinc oxide, cadmium sulfide, and cadmium selenide, are combinations of group II-VI atoms having the wurtzite hexagonal structure. The acoustic velocities vary over a fairly wide range depending upon crystal type and mode of propagation. Coupling factors, k, a measure of the strength of their piezoelectric effect, varies anywhere from 0.13 for the shear k_{15} constant in cadmium selenide up to 0.36 for the k_{33} constant in zinc oxide. Cadmium sulfide has a fairly strong piezoelectric effect and is strongly photoconducting, which made it the prime material for the experimental investigation of electron-phonon interaction phenomena. Zinc oxide is the strongest piezoelectric of the group while retaining a low dielectric constant. This made it a prime candidate for use as a transducer material, and its low acoustic attenuation value is of prime importance for high frequency delay line applications. The wurtzite crystals possess a fairly substantial bandgap and can be obtained in resistivity ranges, which run in general from about one hundredth of an ohm-centimeter up to 10^{10} ohm-centimeters or greater. Their electron mobilities in $cm^2/V\text{-}s$ vary from around 200 in the case of zinc oxide to 600 in the case of cadmium selenide for good crystals.

Gallium arsenide which is a III-V compound having the cubic structure has a smaller bandgap, less resistivity range, but a considerably higher mobility. Its single coupling factor, k_{14}, is comparatively smaller than those of the wurtzite semiconductors. Its mobility and hence resistivity can be controlled with temperature.

All of the compounds in their pure intrinsic states would be classed as insulators. However, their natural growth state leaves them semiconducting because of impurities, the presence of their metallic atoms in interstitial sites and/or a vacancy of the nonmetallic atom. In order to achieve their potential high resistivity state, it is usually necessary to introduce an acceptor impurity or to re-establish stoichiometry by heat treatment in an atmosphere containing the nonmetallic atom. All the crystals were commercially available, and the crystal growers involved were willing to work with the user nies to tailor crystal properties to fit the needs of the individual device manufacturer.

Table I Properties of Piezoelectric Semiconductors

Crystal	Long.Velocity (m/s)	Shear Velocity (m/s)	Long. Atten. (dB/cm)	Long. k	Shear k	Resistive Range (Ohm-cm)	Mobility ($cm^2/V\text{-}s$)
ZnO	6000	2850	0.2	0.36	0.28	$0.01\text{-}10^{12}$	200
CdS	4000	1800	2.5	0.26	0.19	$0.01\text{-}10^{11}$	300
CdSe	3600	1630	7.0	0.19	0.13	$0.05\text{-}10^{10}$	600
GaAs		2900	0.6		0.08	$0.005\text{-}10^{8}$	7000

III. Diffusion Layer Transducer Delay Lines

Work at Bell Laboratories [1] gave rise to a practical type of acoustic delay line using diffusion layer transducers in piezoelectric semiconductors for the generation and detection of the high frequency ultrasonic waves. Fig. 1 shows the four basic parts of the diffusion layer transducer, which also represents the four basic fabrication steps for a delay line. First, an oriented piezoelectric semiconducting crystal of low resistivity is cut in the shape of a rectangular parallelepiped with smooth parallel end faces. Second, an ohmic electrical contact is obtained to the low resistivity body of the crystal. Third, high resistivity transducer regions are diffused at each end of the crystal by using an acceptor impurity. Time and temperature controls are used to regulate the thickness of the resistive region and hence the fundamental frequency. Fourth, a metallic front electrode is placed over the high resistivity region. An RF input across the two metallic layers will present an alternating electric field in the high resistivity diffused region, which generates the ultrasonic wave. Such a transducer is fabricationally simple with good reproducibility and is amenable to low cost semiconductor fabrication processing techniques. Lattice continuity between the transducer and the crystal minimize loss and spurious degradation due to acoustic discontinuities.

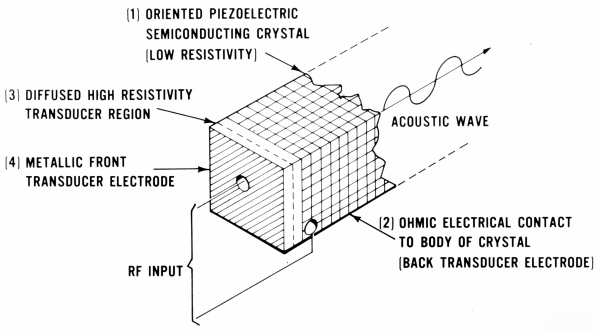

Fig. 1. Diffusion layer transducer geometry.

The diffusion layer transducer was used develop piezoelectric semiconductor delay lines at Motorola for inclusion in electronic systems [2]. The geometry is identical to a conventional two-port acoustic delay line with the transmitting and receiving transducers separated by the acoustic transmission media. The orientation of

crystals sets the mode for excitation and propagation. The length dimension of the crystal sets the delay. Nominal delays of one microsecond correspond to lengths of a quarter inch or less. The cross-sectional dimensions are set by the desired end electrode size. To enhance the transfer of energy from electrical to acoustic modes the end electrodes are reduced in size with increasing frequency to maintain a large value of equivalent acoustic resistance. The electrical distance between body electrodes and the transducer region is made small to keep the in-series resistive losses low.

Group I elements, in general, will act as acceptors in ZnO, CdS, CdSe, and GaAs. A layer of copper vacuum evaporated on the crystals served as the diffusant source for the formation of high resistivity regions in CdS, CdSe, and GaAs. Lithium is used as the diffusant for ZnO from a LiOH paste applied directly on the surface. The range of times and temperatures used for diffusion of the compensating impurities depends upon the appropriate thickness corresponding to the desired fundamental frequency. The temperatures for lithium diffusion in ZnO range from 700^0C for the lowest fundamental transducer frequencies (<100 MHz) to 550^0C for transducer frequencies of 500 to 1000 MHz. Copper diffusion in CdS and CdSe was accomplished at temperatures in the range 300^0C to 500^0C for the VHF region. Copper diffusion in GaAs required diffusion temperatures of 800^0C. The times for diffusion are short, typically from 1 to 5 minutes, and the diffusion process terminated by an air or liquid quench.

There are a number of suitable electrode metals. Body contact metals normally used are Cr-Au to ZnO, Ti-Al to CdS and CdSe and In to GaAs. Care must be taken to assure a good ohmic contact. The transducer end electrodes for CdS, CdSe and GaAs were the residual copper from diffusion, which was overlaid with gold to reduce oxidation. Gold electrodes were used for ZnO.

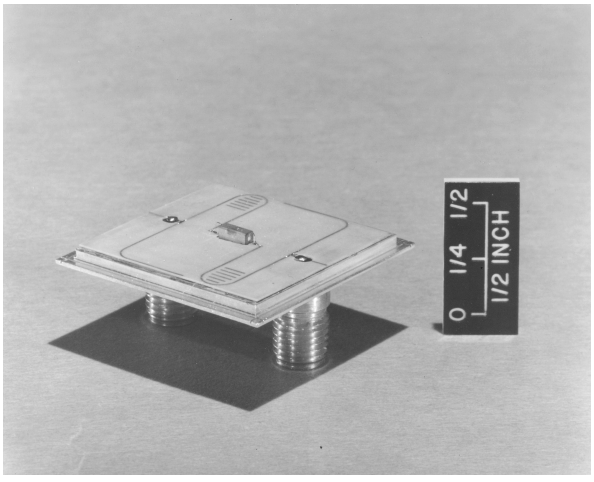

Fig. 2. A 600 MHz 700-nanosecond ZnO delay line with microstrip line matching.

Fig. 2 shows a 700-nanosecond ZnO delay line fabricated for operation at 600 MHz. The delay line crystal was mounted on a 1-inch by 1-inch metallic base plate to which OSM connectors and an alumina substrate with a microstrip line-matching pattern were attached. The microstrip line to the transducer and the stub line to ground were adjusted in length with wire bonds to provide a 50-ohm resistive match to the connectors. The total loss in the delay line was 15 dB at a center frequency of 600 MHz and the 3 dB bandwidth was 120 MHz. At band center where a VSWR near 1.0 was achieved, the spurious signal was 45 dB below the output and was greater than 30 dB over a 500 to 700 MHz band. Direct signal coupling between output and input ports was greater than 60 dB below the delayed signal.

The theoretical and experimental frequency-loss characteristic of a 1-microsecond zinc oxide delay structure is shown in Fig. 3 and is typical of the responses observed with good devices. The experimental points were obtained by impedance matching at each frequency. The minimum loss was 7.0 dB at 450 MHz and the 3 dB bandwidth was 400 MHz. The frequency tuned percentage bandwidths of such delay lines was typically in the range of 70 to 90 per cent. The theoretical curve, shown as a continuous line in Fig. 3, is derived from a simple equivalent circuit model.

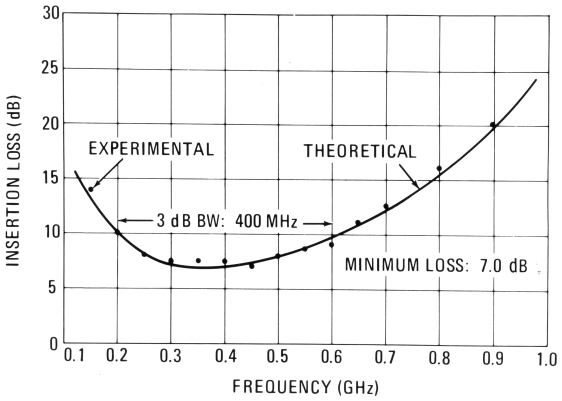

Fig. 3. Frequency characteristic of a ZnO delay line with diffusion layer transducers tuned at each frequency.

IV. The Velocity and Attenuation Due to Electrons in a Piezoelectric Semiconductor

H. D. Nine of General Motors was first to report the effects of the attenuation of ultrasonic waves in CdS through the photoexcitation of electrons [3]. Fig. 4 graphically shows the velocity and attenuation factors of an acoustic wave traveling in a piezoelectric semiconductor. The simplified velocity equation for small signals is given by

$$v=v_o(1+k^2/2\{1+\omega/\omega_d(\Omega)/(1+\Omega^2)\}, \qquad (1)$$

a function of the basic acoustic and semiconducting properties of the crystal and the radial frequency ω. The constant v_o represents the acoustic velocity in a crystal of

high conductivity where the piezoelectric fields are shorted. The k parameter is the electromechanical coupling coefficient and ω_d is the diffusion frequency. The value Ω equals $(\omega_c/\omega+\omega/\omega_d)$ where ω_c is the dielectric relaxation frequency, which is the conductivity of the crystal divided by its dielectric constant. The diffusion frequency is the ratio of the acoustic velocity squared divided by the diffusion constant. The diffusion constant D involves the factors of charge, mobility, the Bolztmann constant, temperature, and a factor f related to the fractional amount of free carriers participating in the interaction. The upper part of Fig. 4 shows the velocity effect, which the conductivity (or frequency) has on an acoustic wave traveling in the piezoelectric semiconductor. For the case of high conductivity or low frequency the velocity has the value v_o. For very low conductivity (high resistivity) the velocity has a value $(1+k^2/2)$ times higher. In the vicinity where the radial frequency equals the dielectric relaxation frequency $(\omega=\omega_c)$ the velocity change occurs. This represents a simple relaxation phenomenon, which is characteristic of piezoelectric semiconductors.

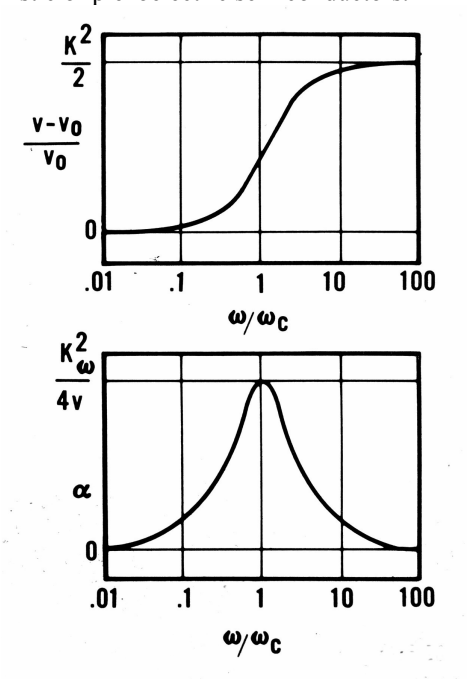

Fig. 4. Velocity and attenuation characteristics of an acoustic wave traveling in a piezo-semiconductor.

The expression for the attenuation factor and its behavior are shown at the bottom of Fig. 4. Its equation is given by

$$\alpha = k^2\omega/2v\{(\omega_c/\omega)/(1+\Omega^2)\}. \qquad (2)$$

The attenuation expression involves the same basic factors and displays a relaxation phenomenon whose strength is directly proportional to electromechanical coupling factor and frequency and inversely proportional to the acoustic velocity. For the case of high conductivity, the attenuation due to the presence of charge carrier in the crystal is very small and any observed attenuation would primarily be due to other processes such as phonon interactions. As the conductivity approaches the condition where the radial frequency of the acoustic wave is the same as the dielectric relaxation frequency $(\omega=\omega_c)$ a strong attenuation of the wave occurs due to the presence of electrons. The maximum attenuation due to electron-phonon interaction is equal to $k^2\omega/4v$. Finally, going to a condition which would be characterized by high resistivity or very high frequency the attenuation returns to its background level.

These effects have been measured in crystals of ZnO, CdS, CdSe, and GaAs. The effects are very readily demonstrated in cadmium sulfide where the crystal conductivity may be controlled over a very large range by incident light (the photoconductive effect). The electron-phonon interaction effect can be used as a basic tool for measurement of the electromechanical coupling factor by either absorption or velocity changes.

Fig. 5 shows the oscilloscope presentation of a pulse echo pattern depicting the velocity dispersion in CdS under the condition of high and low resistivity. The measurements were made at 30 MHz, the time scale is 1 μsec per major division, and the pulses shown were toward the end of the echo pattern. The crystal was highly photoconductive. An echo pattern could be obtained by darkening the crystal (high resistivity) to obtain the fast wave velocity v_{oo} and then by shining an intense incandescent light on the crystal an echo pattern representing the condition of low resistivity (slow wave velocity v_o) could be observed. The displacement of the pulses is seen in the scope trace with the amplitudes approximately equal. Several round trips are represented, hence the substantial separation of pulses. The change in velocity with conductivity change can be plotted, but the entire dispersion curve cannot be traced, because of the strong pulse attenuation. At low frequencies with a short crystal the entire dispersion relation can be seen.

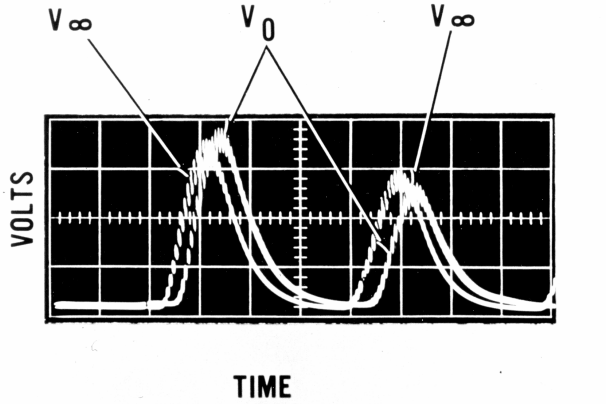

Fig. 5 Pulse echo pattern showing velocity dispersion in CdS. Amplitude: 0.5 V per large division, Time: 0.2 μs per large division.

An example of the attenuation property is shown in Fig. 6 for gallium arsenide. The room temperature resistivity of the gallium arsenide was 2000 ohm-centimeters, and the mobility was 4000 centimeters per volt second. The experiment was carried out on a [110] oriented GaAs crystal 1 cm in length at a frequency of 82 MHz. Y-cut quartz bonded transducers were used to excite and detect the ultrasonic shear waves. Changing the temperature could vary the conductivity of the crystal. Conditions representing a ratio of radial frequency to dielectric relaxation frequency of 100 down to 0.4 could be obtained. The observed attenuation in gallium arsenide follows the expected theoretical dependent, and the data could be fitted to a theoretical curve in which a coupling factor, k_{14} = 0.085 was used. This value is close to the value of k_{14} = 0.075 which has been measured by other techniques. A maximum acoustic attenuation of 14 dB/cm was observed at ω/ω_c = 1. The background attenuation due to other processes was approximately 0.5 db/cm.

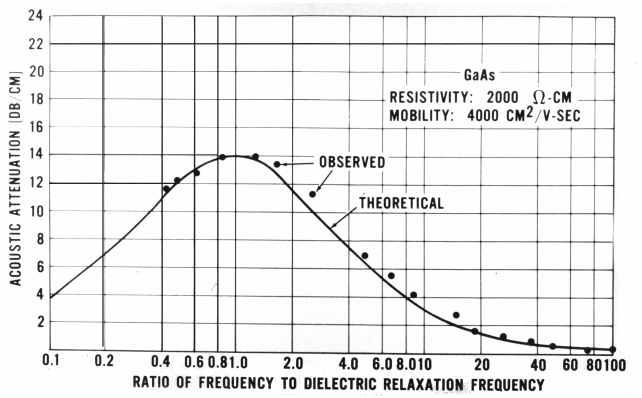

Fig. 6 Attenuation of acoustic waves in GaAs in dB/cm as a function of ω/ω_c.

V. The Interaction of Acoustic Waves and Electrons in a Piezoelectric Semiconductor under Applied Field.

Now we shall consider what happens when a dc electric field is applied to the semiconductor in the presence of an acoustic wave and charge carriers [4,5]. The equations now contain a field factor gamma, γ, which is defined as 1 minus the product of mobility and electric field strength (electron drift velocity) divided by v_0, the velocity of the acoustic wave (γ=1-$\mu E/v_0$). The field dependent behavior of the velocity is shown in the upper graph of Fig. 7 with the normalized velocity difference plotted as a function of gamma. For large positive or negative values of gamma (high field strength) the acoustic wave velocity is equal to v_0 (1 + $k^2/2$). At the point where the electric field is zero (no electron drift velocity (γ = 1)), the velocity expression becomes that given in Eq. 1, and there is a reduction in velocity from its high field value. In the region where gamma is equal to zero, the case where the drift velocity v_d is equal to the acoustic velocity, there is a substantial velocity change with a minimum value at γ = 0, and the velocity approaches v_0. Physically, as the electron drift velocity approaches that of the acoustic wave, the wave velocity is decreased, reaches a minimum when electron velocity equals acoustic velocity, and then increases back to the high field value for electron drift velocities greater than the acoustic velocity.

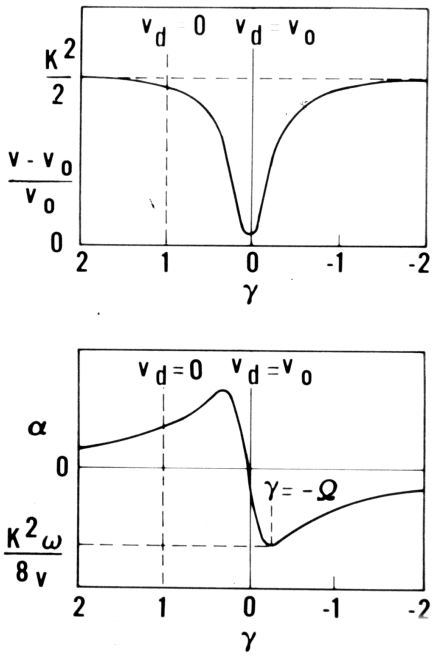

Fig. 7. Velocity and attenuation characteristics of a piezo-semiconductor under an applied electric field E, where γ = 1- $\mu E/v_0$.

The attenuation relation is also shown graphically in Fig. 7. For high positive or negative fields the attenuation due to electron-phonon interaction becomes zero. When γ = 1 (no applied field) the attenuation due to charge carriers is that of equation 2. As the electron velocity approaches the acoustic wave velocity the attenuation increases, goes to a maximum and then to zero attenuation when drift velocity equals acoustic wave velocity. When electron drift velocity exceeds the acoustic wave velocity the attenuation is negative, and there is gain reaching a maximum value when the field parameter gamma is equal to minus Omega. Omega is the ratio of dielectric relaxation frequency to the frequency plus the ratio of frequency to the diffusion frequency. Thus, when the charge carriers are traveling at a velocity less than the acoustic wave, there is strong wave attenuation, but when the velocity of the electrons exceeds that of the acoustic wave, energy is given from the electrons to the acoustic wave through the piezoelectric field causing it to amplify. This effect is the basis of the ultrasonic amplifier and electro-acoustic effects used to develop active devices for prototype electronic systems.

Figure 8 shows schematically the dependence of attenuation in a piezoelectric semiconductor on frequency, ω, and electron drift field E. The reference point is taken as $\omega=\sigma/\varepsilon$ and E = 0; positive attenuation is in the vertical, increasing frequency out and down to the left and increasing electron drift field to the right. Contour lines representing a three-dimensional map of the dependencies discussed are shown in this figure. The influence of conductivity and field on attenuation may be qualitatively visualized. For example, at very high, or very low frequencies compared to the conductivity frequency, there will be no attenuation effect. The attenuation is most pronounced along the σ - E axis ($\omega = \sigma/\varepsilon$) where strong positive and negative attenuation regions are present. We shall now consider experimental evidence of the attenuation as a function of field.

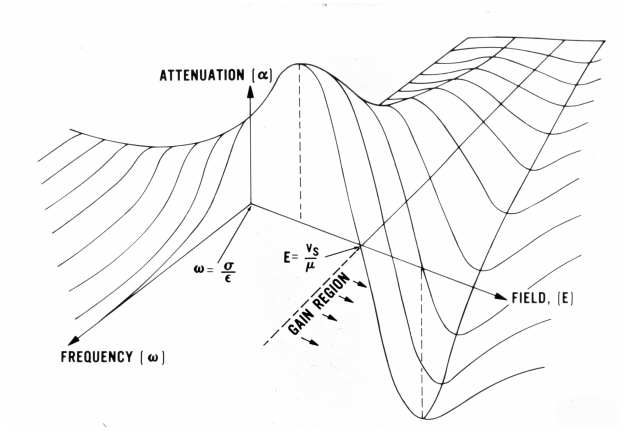

Fig. 8. Attenuation in a piezo-semiconductor as a function of frequency, ω, and electron drift field E.

In order to observe the electroacoustic effect acoustic transmission structures consisting of a parallelepiped cut crystal of the piezoelectric semiconductor, an ohmic metallic contact placed on each end of the crystal, and a quartz transducer buffer rod bonded with quartz wax on each end of the crystal. The dc voltage is applied across the crystal and can be varied or reversed in polarity to produce different field intensities. The acoustic wave is generated and detected by the transducers and changes in intensity due to field, or conductivity changes may be observed.

Fig. 9 shows experimental data on the electroacoustic interaction in gallium arsenide as a function of field and resistivity [6]. The GaAs was cut for shear wave propagation along the (110) direction with particle displacement in the (001) direction. The sample was a rectangular shaped parallelepiped with cross-sectional dimensions normal to the direction of acoustic propagation of 3.4 mm x 3.4 mm. The length of the crystal along the (110) direction was 13.6 mm. Y-cut quartz transducers with a fundamental frequency of 60 Mc/s were epoxy bonded directly to the GaAs. Prior to bonding, indium was evaporated at each of the crystals and diffused to form an ohmic contact region for the bias field. The operating conditions under which the evaluations was made are as follows: Operating frequency, 60 MHz, RF pulse width, 1.2 μs, dc pulse width, 5.2 μs, pulse repetition rate, 80 pps, RF input level, 300 mV, dc bias field, ± 1000 V/cm.

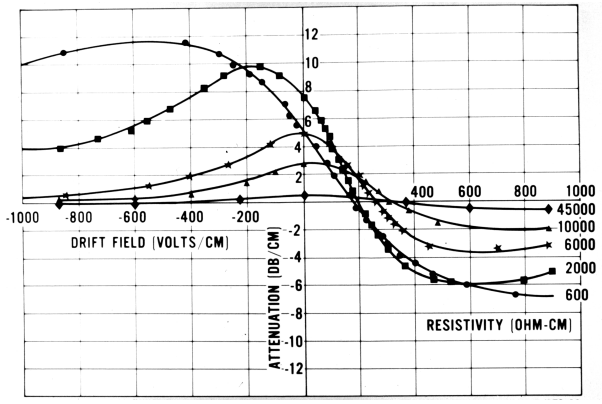

Fig. 9. The electroacoustic interaction in gallium arsenide as a function of field and resistivity.

The resistivity of the GaAs was temperature-dependent exhibiting a linear characteristic with inverse absolute temperature when plotted on semi-log paper. Data was taken in the temperature range from 0°C to 60°C with a resulting resistivity change from 45,000 ohm-cm to 600 ohm-cm. This permitted an evaluation of the electro-acoustic gain interaction is the range $0.01 < \omega_c/\omega \leq 4$. The change in attenuation with field and resistivity is in general agreement with theory. A true antisymmetric attenuation characteristic about the threshold field for the onset of gain is not strictly observed. In the forward field direction, the negative attenuation has a broad maximum, whereas a more pronounced maximum in the attenuation characteristic is observed in the reverse field direction. The positive attenuation under reverse bias is greater than the acoustic gain (negative attenuation) under forward bias at these maxima. It was also observed that the threshold field for the onset of acoustic gain decreases with decreasing resistivity. In this material, the effective drift mobility as determined from the crossover field increased from 1120 cm^2 / V-s to 2000 cm^2 / V-s as the resistivity decreased from 45,000 ohm-cm to 600 ohm-cm. This is a factor of from 2 to 4 below the measured hall mobility. Similar field-dependent characteristics of the acoustic attenuation were also observed with CdS. By taking into account the effects of carrier trapping on the interaction, the observed behavior can be accounted for. From the asymmetry the relaxation time for electron trapping can be calculated, and for the GaAs used here was in the range 2.0×10^{-9} to 9×10^{-9} seconds.

Figure 10 shows the type of interaction characteristic observed in a very high quality CdS crystal. The data was taken on an oriented crystal for shear wave propagation 0.5 cm in length and 0.2 by 0.2 cm in cross-section. Y cut quartz transducers with a fundamental frequency of 84 MHz were bonded over Ti-Al ohmic contracts at each end of the crystal. They were oriented for particle displacement of the acoustic wave along the C-axis of the CdS. The data shown in the figure was measured at a constant resistivity level of 8000 ohm-cm. The drift mobility of the crystal was 270 cm^2 /V-s. The forward and reverse attenuation characteristics are plotted as a function of drift field intensity. The reverse field direction data is shown folded back. The zero field attenuation level is established by darkening the crystal. The data is taken with pulsed RF and dc fields.

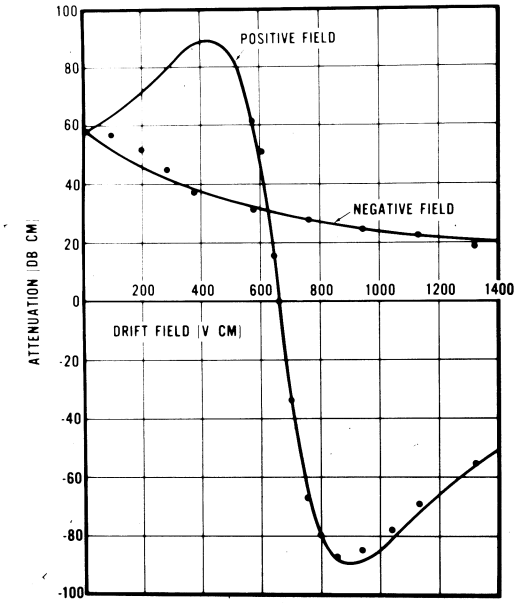

Fig. 10 Attenuation characteristic in dB/cm of CdS crystal as a function of drift field in V/cm at 84 MHz.

The attenuation characteristic shows a very symmetric behavior, which can be adequately described using simple linear theory. The behavior is indicative of a crystal free of major trapping centers or imperfections. Maximum negative and positive attenuation values are 90 dB/cm. The one-half centimeter length crystal gave an electroacoustic gain of 45 dB and an attenuation change of 90 dB. High quality cadmium sulfide produced the best experimental gain results reported in the literature.

Table II summarizes the experimental results of work on the strength of the electroacoustic gain interaction observed in piezoelectric semiconductors at Motorola. Experimental and theoretical values are given. The theoretical value of gain factor is for the shear mode of operation. Amplification in CdS has been observed over a fairly wide range of frequencies. For cadmium sulfide, acoustic gain values as high as 425 dB/cm have been observed at frequencies in the UHF region. The experimentally observed db per centimeter per megahertz gain factor, which theoretically is 2.9, drops in value as one goes higher in frequency. The theoretical value can almost be reached at low frequencies. In the case of gallium arsenide and cadmium selenide, the gain factors were much lower than theoretical. Work at Stanford on GaAs at frequencies of 1 GHz has given a gain factor of 0.07 db/cm-MHz. The zinc oxide data shown in the Table is based on experiments in which the acoustic noise is allowed to be amplified. The observed gain factor was down by a factor of 10 from theoretical. Although zinc oxide is a much more difficult material to work with, theoretically gain factors of around 3.4 db per centimeter per megahertz would be expected at low frequencies. Work at both Minnesota Mining and Manufacturing Microwave Electronics has been carried out on amplification in ZnO. The work at 3M gave a 52 db/cm gain at 30 MHz using longitudinal waves. This is a gain factor of 1.7 db/cm-MHz. At MEC gains of 25 db were observed in the 0.6 to 2.5 GHz region with longitudinal waves. This gives a gain factor of less than 0.04 dB/cm/MHz.

Table II. Realized Gain in an Ultrasonic TWA

Crystal	Freq. (MHz)	Gain (dB/cm)	Gain Factor (dB/cm-MHz)
CdS	60	150	2.5
	200	305	1.7
	550	425	0.8
	1000	300	0.3
GaAs	30	3	0.1
	92	9	0.1
CdSe	45	15	0.3

Figure 11 shows the progression of ultrasonic traveling wave amplifiers as they evolved at Motorola. On the right is the first amplifier, which the configuration often used in evaluation of material. Quartz transducers are bonded onto fused quartz rods, and then the cadmium sulfide crystal is between the rods. A nonpermanent-bonding agent such as quartz wax or a resin is used for the case of evaluating the gain interactions. In the amplifier configurations shown here, permanent epoxy bonds were used.

The first large net gain values were obtained in 1963 with the device on the left in which the based quartz buffer rods are eliminated and quartz transducers bonded directly on the centimeter long cadmium sulfide crystal [7]. This amplifier had a net gain of 40 db under pulsed operation at 60 MHz. The total acoustic gain observed was 75 db with the difference of 35 db attributed to loss in the transducers and the background propagation loss in the crystal.

The last amplifiers that were made resulted from 3 years of work on materials and packaging and an example is shown between the two larger amplifiers. These amplifiers showed large pulse gains and were heat sunk to permit high duty cycle operation. The net gain values of the amplifiers were no greater than those observed earlier, but an interrupted cw operation of up to 90% was obtained. The amplifier had permanently bonded quartz transducers with CdS crystal conductivity controlled by an internal light.

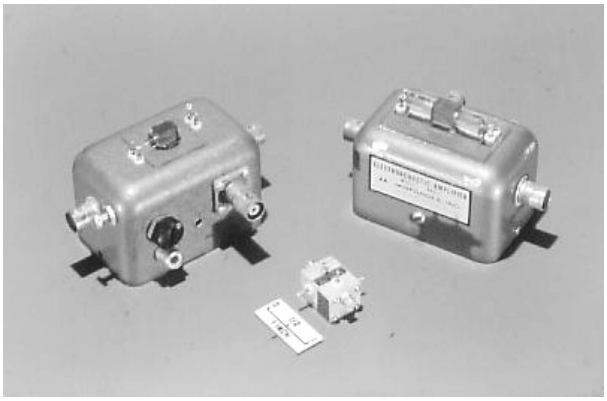

Fig. 11. Ultrasonic traveling wave amplifiers.

VI. Current Oscillations in Piezo-semiconductors

There are some interesting effects in piezoelectric semiconductors, which can be observed under the presence of a dc electric field and its influence on the natural thermal vibrations in the material [8]. These acoustoelectric effects can be seen in the voltage-current characteristics, and Figure 12 shows two typical types observed. The oscilloscope traces show current pulses as a function of time and a corresponding measured I-V characteristic. Up to the point where the electron drift velocity, v_d, is less than the sound velocity, v_s, the voltage current relation follows Ohms Law. For field values beyond this point nonohmic behavior is observed resulting in a current saturation, which may be strong or weak, and often current oscillations indicated by the oscilloscope traces. The top trace shows a strong saturation of the average current value and current oscillations. Each trace corresponds to a point on the graph. In the lower trace the current deviation is less and for high enough fields the ohmic condition is restored. The deviations observed can be explained qualitatively from the attenuation versus field characteristic of acoustic waves in piezoelectric semiconductors. The bias field initiates traveling acoustic domains, which account for the current oscillations dependent on crystal length. Considerable work was done on the observation of these effects in piezoelectric crystals and oscillators were developed.

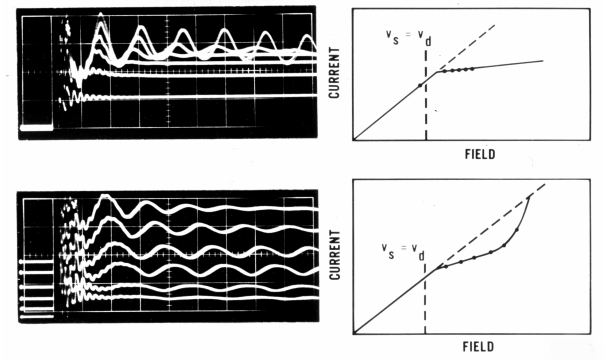

Fig. 12. Current saturation and oscillations in CdS under an increasing bias field.

Figure 13 shows a simple oscillator, which was made using the current oscillation effect. The oscillator was built using a CdS crystal approximately 2 millimeters in length, 0.4 mm in thickness and 1.3 mm in width. The CdS is mounted directly on a BeO substrate for heat sinking with terminals for the applied field and a capacitive coupling for the oscillatory output. This device put out a 1 MHz signal of 430 milliwatts with an efficiency of approximately 2%. It represents a very small compact solid-state oscillator using acoustic transit time modes.

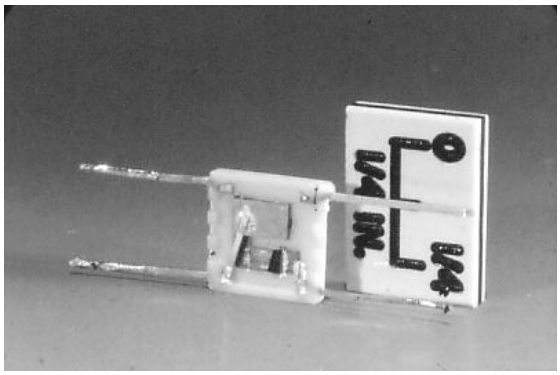

Fig. 13. CdS oscillator operating at 1 MHz.

VII. Conclusion

While this trip down memory lane could be viewed as a technology, which shone brightly with great device potential and then flamed-out, it is a page of history, which during the sixties captured the imaginations of workers in ultrasonics and electronics. The advances that are made in solid-state electronics are often limited by the basic properties of the materials themselves. This is especially true for the piezoelectric semiconductor where a large number of exciting acoustoelectronic, (AE), devices lay in wait for those elusive ideal materials, which on the theoretician's paper performed admirably. The majority of the work with acoustic effects in piezoelectric semiconductors was devoted to explaining experimental deviation from theory and the observation and analysis of effects due to imperfect crystals. The 1965 Special issue on Ultrasonics of the Proceedings of the IEEE featured on its cover a depiction of the ultrasonic traveling wave

amplifier [9]. W.H Haydl has provided a substantial biography of the work with semiconducting piezoelectric crystals in his Stanford Ph.D. dissertation [10].

The sixties were also characterized by the tension, which developed between the so-called functional analog device and the integrated digital circuit. There were several analog effects in solids that commanded the attention of the device designer. As the digital devices and integrated circuits improved in efficiency and capability, they over-shadowed the functional device concepts. In the case of the acoustic device development using piezoelectric semiconductors, they became over-shadowed by surface acoustic wave, SAW, devices. It is interesting to note that there was a carryover of the basic concept of a shorted and open piezoelectric field into SAW device development. Metal layers on piezoelectric substrates were used to split the generated surface wave front with 180° phase shift so as to suppress bulk wave modes in SAW filters [11]. Ultra-thin metal layers could be used to attenuate surface acoustic waves through the acoustoelectric interaction as a cleaner alternative to soft dampening material [12]. There were film layers and separated media SAW amplifiers in which the electron flow was in a semiconducting material deposited in the region between the interdigital transducer electrodes or brought into proximity to the piezoelectric crystal [13]. The SAW delay line became a direct replacement for the resistive or diffusion layer delay line. By 1969 the special issue on microwave acoustics of the IEEE Transactions of the MTT Society featured more articles on SAW than BAW devices [14].

The sixties were an exciting time to be in the acoustic wave device business for researchers in universities, government laboratories, and industry. Several dissertations resulted from the investigation of acoustoelectronic effects. Government laboratories made funding available to the defense industry. Manufacturers improved the properties of their piezoelectric semiconductor crystals as the device developers sought to attain near theoretical results. The net gain was a greater understanding of the theoretical and experimental capabilities of using piezoelectric semiconductors for application as devices in electronic systems.

Acknowledgments

The work reported in this paper involved a number of co-workers at Motorola over the decade of the sixties. Engineering contributions were made by D. E. Allen, W.H. Brendecke, P. L. Clar, and N. G. Sakiotis. Fabrication, testing, and data analysis involved the skills of M. D. Adamo, J. W. Brewer, G. Ehlenberger, J. A. Grosberg, W. R. Gayton, T. McCloskey, C. M. Munoz, W. J. Neubert, G. Nowik, M. J. Shaw, and H. W. Spears. The cooperation of the crystal manufacturers was very important; Eagle Picher for CdS, Harshaw Chemical for CdS and CdSe, Monsanto for GaAs, and Minnesota Mining for ZnO. The crystal manufacturers were very willing to provide crystals with the necessary characteristics to optimize the required interactions. Finally it was through the foresight of Nicholas G. Sakiotis that the work was initiated at Motorola and the first definitive results on a 60 MHz 40 dB net gain amplifier were presented at the 1963 IEEE Ultrasonics Symposium in Washington D. C., 40 years ago.

References

[1] D. L. White, “The depletion layer and other high-frequency transducers using fundamental modes,” in *Physical Acoustics, Principles and Methods*, vol. I part B, W. P. Mason, Ed., New York, Academic Press, 1964, pp. 321-352.

[2] F. S. Hickernell, “Piezoelectric semiconductor acoustic delay lines,” IEEE Trans. on Microwave Theory and Tech. vol. 17, pp. 957-963, November 1969.

[3] H. D. Nine, “Photosensitive ultrasonic attenuation in CdS,” Phys. Rev. Letters, vol. 4, p. 359, 1960.

[4] D. L. White, “Amplification of ultrasonic waves in piezoelectric semiconductors,” J. Appl. Phys. Vo. 33, pp. 2547-2554, August 1962.

[5] J. H. McFee, “Transmission and amplification of acoustic waves in piezoelectric semiconductors,” in *Physical Acoustics, Applications to Quantum and Solid State Physics*, vol. IV part A, W. P. Mason, Ed., New York, Academic Press, 1966, pp. 1-45.

[6] F. S. Hickernell, "The Electroacoustic Gain Interaction in III-V Compounds: Gallium Arsenide," IEEE Trans. on Sonics and Ultrasonics, vol. 13, pp. 73-77, July 1966.

[7] F. S. Hickernell and N. G. Sakiotis, "An Electroacoustic Amplifier with Net Electrical Gain," Proceedings of the IEEE, vol. 52, p. 194, February 1964.

[8] R. W. Smith, “Current saturation in piezoelectric semiconductors,” Phys. Rev. Letters, vol. 9, pp. 87-90, August 1962.

[9] Proceedings of the IEEE, *Special Issue on Ultrasonics*, vol. 53, October 1965.

[10] W. H. Haydl, “Current instabilities in piezoelectric semiconductors,” M. L. Report No. 1517, Microwave Laboratory, W. W. Hansen Laboratories of Physics, Stanford University, March 1967.

[11] C. T. Vasile and R. LaRosa, “Broadband bulk-wave cancellation in acoustic-surface wave devices,” Electron. Lett. Vol. 8, pp. 478-480, 1972.

[12] P. Bierbaum, Interaction of ultrasonic surface waves with conduction electrons in thin metal films,” Appl. Phys. Lett., vol. 21, pp.595-598, 1972.

[13] K. M. Lakin and H. J. Shaw, “Surface wave delay line amplifiers,” IEEE Trans. on Microwave Theory and Tech. Vol. 17, pp. 912-920, November 1969.

[14] IEEE Trans. on Microwave Theory and Tech., *Special Issue on Microwave Acoustics*, vol. 17, November 1969.